Substitutions of Conserved Aromatic Amino Acid Residues in Subunit I Perturb the Metal Centers of the Escherichia coli bo- Type Ubiquinol Oxidase †

ARTICLE *in* BIOCHEMISTRY · MARCH 1998

Impact Factor: 3.02 · DOI: 10.1021/bi971978k · Source: PubMed

10 AUTHORS, INCLUDING:

Tatsushi Mogi
Medical & Biological Laboratories Co., Ltd.
153 PUBLICATIONS **4,411** CITATIONS
SEE PROFILE

Jun Minagawa
National Institute for Basic Biology
62 PUBLICATIONS **2,552** CITATIONS
SEE PROFILE

Motonari Tsubaki
Kobe University
104 PUBLICATIONS **2,142** CITATIONS
SEE PROFILE

Hiroaki Nakamura
National Institute for Fusion Science
261 PUBLICATIONS **1,991** CITATIONS
SEE PROFILE

Substitutions of Conserved Aromatic Amino Acid Residues in Subunit I Perturb the Metal Centers of the *Escherichia coli bo*-Type Ubiquinol Oxidase[†]

Tatsushi Mogi,*[,‡] Jun Minagawa,[‡,§] Tomoyasu Hirano,[‡] Mariko Sato-Watanabe,[‡] Motonari Tsubaki,[||] Tadayuki Uno,[⊥] Hiroshi Hori,[Δ] Haruki Nakamura,[○] Yoshifumi Nishimura,[▽] and Yasuhiro Anraku[‡]

Department of Biological Sciences, Graduate School of Science, University of Tokyo, Hongo, Bunkyo-ku, Tokyo 113, Department of Life Sciences, Faculty of Science, Himeji Institute of Technology, Kamigoori-cho, Akou-gun, Hyogo 678-12, Faculty of Pharmaceutical Sciences, University of Kumamoto, Ohehon-machi, Kumamoto, Kumamoto 862, Department of Biophysical Engineering, Faculty of Engineering Science, University of Osaka, Toyonaka, Osaka 560, Department of Bioinformatics, Biomolecular Engineering Research Institute, Furuedai, Suita, Osaka 565, and Graduate School of Integrated Science, Yokohama City University, Seto, Kanazawa-ku, Yokohama 236, Japan

Received August 11, 1997; Revised Manuscript Received December 14, 1997

ABSTRACT: Cytochrome *bo* is a four-subunit quinol oxidase in the aerobic respiratory chain of *Escherichia coli* and functions as a redox-coupled proton pump. Subunit I binds all the redox metal centers, low-spin heme *b*, high-spin heme *o*, and Cu_B, whose axial ligands have been identified to be six invariant histidines. This work explored the possible roles of the aromatic amino acid residues conserved in the putative transmembrane helices (or at the boundary of the membrane) of subunit I. Sixteen aromatic amino acid residues were individually substituted by Leu, except for Tyr^{61} and Trp^{282} by Phe and Phe^{415} by Trp. Leu substitutions of Trp^{280} and Tyr^{288} in helix VI, Trp^{331} in loop VII−VIII, and Phe^{348} in helix VIII reduced the catalytic activity, whereas all other mutations did not affect the in vivo activity. Spectroscopic analyses of the purified mutant enzymes revealed that the defects were attributable to perturbations of the binuclear center. On the basis of these findings and recent crystallographic studies on cytochrome *c* oxidases, we discuss the possible roles of the conserved aromatic amino acid residues in subunit I of the heme−copper terminal oxidases.

Cytochrome *bo* is a four-subunit quinol oxidase in the aerobic respiratory chain of *Escherichia coli* (*1, 2*) and generates an electrochemical proton gradient across the cytoplasmic membrane via not only the scalar protolytic reactions but also redox-coupled proton pumping (*3, 4*). Molecular biological and spectroscopic studies have shown that it belongs to the heme−copper respiratory oxidase superfamily (*5, 6*). Therefore, the structure of redox metal centers in subunit I and mechanism of proton pumping appear to be essentially the same in quinol oxidases and bacterial and mammalian cytochrome *c* oxidases.

Site-directed mutagenesis studies on subunit I (the *cyoB* gene product) have demonstrated that low-spin heme *b* (cytochrome $b_{563.5}$) is ligated by His^{106} (in transmembrane helix II) and His^{421} (X), high-spin heme *o* (cytochrome *o*) by His^{419} (X), and Cu_B by His^{284} (VI) and His^{333} and His^{334} (loop VII−VIII) (see refs *7* and *8* for reviews). Heme *o* and Cu_B are antiferromagnetically coupled and form a heme−copper binuclear center where reduction of molecular oxygen takes place (*9, 10*). Recent X-ray crystallographic studies on cytochrome *c* oxidases (*11, 12*) confirmed the axial ligands of the metal centers; however, His^{333} and His^{334} were found in loop VII−VIII (Trp^{331}−Gly^{341}) instead of helix VII (Leu^{316}−Ala^{340}) in our working model for the redox metal centers, which consists of a bundle of transmembrane helices, II, VI, VII, VIII, and X (*8, 13*) (Figure 1).

Substrates are oxidized at the low-affinity quinol oxidation site (Q_L)[1] in subunit II, and then electrons are transferred to the binuclear center through the high-affinity quinone binding site (Q_H) and heme *b* (*14*−*18*). Electron transfer in subunit I seems to be mediated via a covalent bond system consisting of side chains of heme ligands and the connecting peptide backbone His^{421}-Phe^{420}-His^{419} (*8, 19*). Side chains of the conserved aromatic amino acid residues may participate in long-range electron transfer between the metal centers (*20, 21*) or provide a binding pocket for the prosthetic groups (*22*).

In this study, we replaced 16 conserved aromatic amino acid residues in subunit I with Leu, Phe, or Trp and examined their effects on the catalytic activity and the redox metal centers. On the basis of present observations, we discuss

[†]This work was supported in part by Grants-in-aid for Scientific Research on Priority Areas (08249106 and 09257213), for Scientific Research (B) (08458202), and for Exploratory Research (08878097) from the Ministry of Education, Science, Sports and Culture, Japan. This is paper XXVIII in the series Structure−function studies on the *E. coli* cytochrome *bo*.

* To whom correspondence should be addressed: Fax 81-3-3814-2583; E-mail mogi@biol.s.u-tokyo.ac.jp.

[‡] University of Tokyo.

[§] Present address: Institute of Physical and Chemical Research (RIKEN), Hirosawa, Wako, Saitama 351-01, Japan.

[||] Himeji Institute of Technology.

[⊥] University of Kumamoto.

[Δ] University of Osaka.

[○] Biomolecular Engineering Research Institute.

[▽] Yokohama City University.

[1] Abbreviations: Q_L, low-affinity quinol oxidation site; Q_H, high-affinity quinone binding site; EPR, electron paramagnetic resonance; FTIR, Fourier transform infrared spectroscopy; Q_1H_2, ubiquinol 1; HPLC, high-performance liquid chromatography; WT, wild-type.

S0006-2960(97)01978-8 CCC: $15.00
Published on Web 01/22/1998

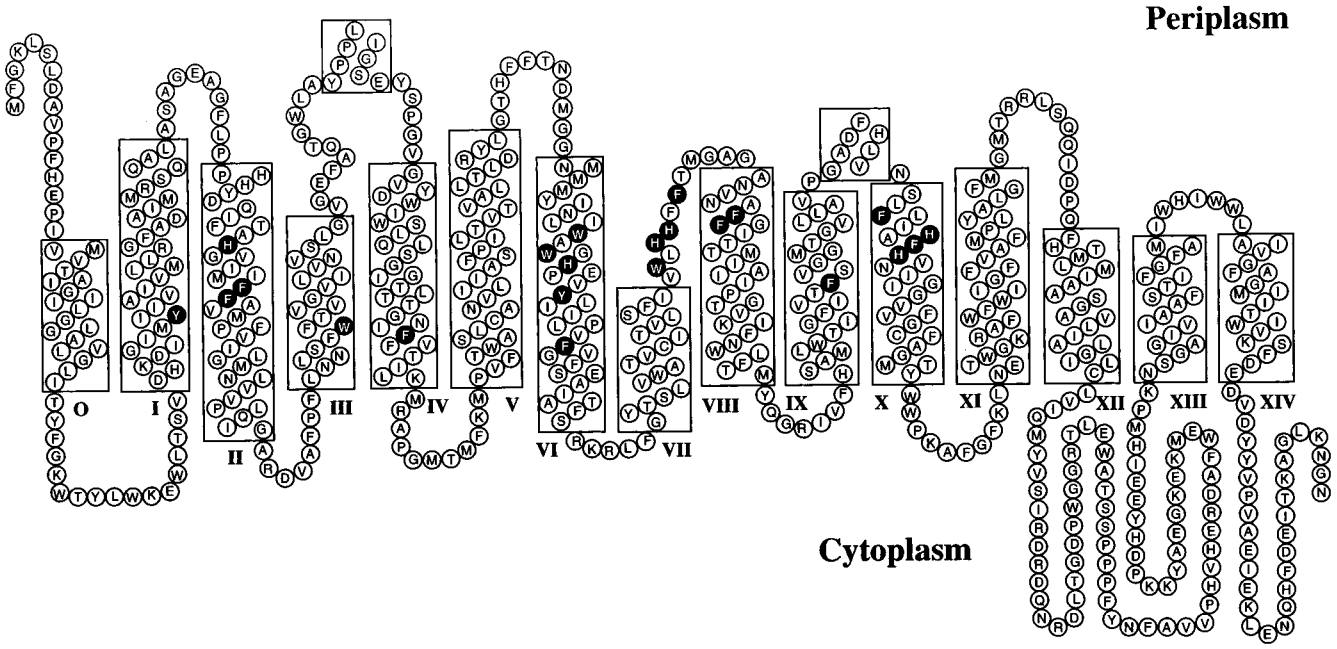

FIGURE 1: Secondary structure model of subunit I showing locations of the conserved aromatic residues altered in this study. The previous model (*13*) was modified on the basis of the X-ray structure of cytochrome *c* oxidase from *Paracoccus denitrificans* (*11*). Transmembrane helices are indicated by rectangles. Locations of the conserved aromatic amino acid residues examined in this study and the six invariant His residues, which function as the axial ligands of the prosthetic groups, are shown as black circles.

the possible role of the conserved aromatic amino acid residues in subunit I of the heme−copper terminal oxidases.

MATERIALS AND METHODS

Introduction of Gene-Engineered Restriction Sites in Subunit I Gene. To facilitate mutagenesis and sequencing analysis of the subunit I (*cyoB*) gene, we created five unique restriction sites in the wild-type gene by site-directed mutagenesis using oligonucleotide primers (22 nucleotides on average) (*13*). Thus, *Apa*I (nucleotide number 1657[2]), *Xho*I (1927), *Mlu*I (2046), and *Eco*81I (2333) sites (Figure 2) were sequentially introduced into the *cyoB* gene on phagemid pCYOF4 (*13*), which contains the gene-engineered *Nhe*I site at the 3′-end of the subunit II (*cyoA*) gene. In addition, one of two *Hin*dIII sites (1444) was eliminated from the *cyoB* gene (Figure 2). Subsequently, the nucleotide sequence of the resultant phagemid, pCYOF9, was confirmed by direct plasmid sequencing (*13*). Finally, the *Afl*III−*Spl*I fragment of pCYOF9 was subcloned into the corresponding site of a single-copy expression vector, pMFO4 (*13*), which carries the entire wild-type *cyo* operon. The resultant plasmid, pMFO9, contains six gene-engineered unique restriction sites, *Nhe*I, *Apa*I, *Xho*I, *Mlu*I, *Eco*81I, and *Hin*dIII, in the *cyo* operon.

Construction of Subunit I Mutants. Sixteen aromatic amino acid residues conserved in transmembrane helices of subunit I (Figure 1) were individually replaced with Leu, except for Tyr^{61} and Trp^{282} with Phe and Phe^{415} with Trp, by site-directed mutagenesis using mutagenic primers (21 nucleotides on average). pCYOF9 DNA was isolated from each candidate mutant clone and the nucleotide sequence of the small restriction fragments (Figure 2) containing the desired codon change (TTG for Leu, TTT for Phe, and TGG for Trp) was confirmed by direct plasmid sequencing. Then these fragments were replaced with their counterparts in the wild-type pCYOF9 and the nucleotide sequences corresponding to these fragments in the recombinant plasmids were again confirmed by DNA sequencing. For expression of the mutant *cyo* operon, the *Nhe*I−*Eco*RI fragment of the mutant pCYOF9 DNAs (Figure 2) was replaced with the counterpart of the wild-type pMFO4 to produce the pMFO9 derivatives.

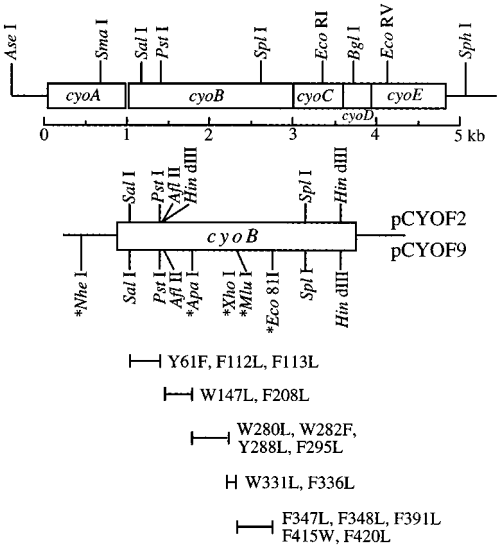

FIGURE 2: Physical map of the *cyo* operon in phagemid pCYOF9. Coding regions of the *cyo* genes are shown by open *rectangles*. The gene-engineered *Nhe*I, *Apa*I, *Xho*I, *Mlu*I, *Eco*81I, and *Hin*dIII sites were introduced by site-directed mutagenesis without any amino acid change in subunits I and II and are marked by asterisks. The unique restriction sites present in the native gene are shown above the rectangles, and the gene-engineered restriction sites in pCYOF9 are shown below the rectangles. Restriction fragments used for sequencing analysis and subcloning are shown by horizontal *lines*.

[2] Nucleotide number is based on a mRNA start point of the *cyoABCDE* operon (*23*).

Determination of Doubling Time of Mutants. Doubling time of the mutants was determined in liquid culture as follows. A terminal oxidase-deficient strain ST2592 (Δ*cyo* Δ*cyd recA*) was anaerobically transformed with the mutant pMFO9. A single colony on a Luria broth−15 μg/mL ampicillin−0.5% glucose plate was inoculated in 5 mL of minimal medium A (*24*) containing 15 μg/mL ampicillin and 0.5% glucose and was allowed to grow anaerobically at 37 °C overnight. Cells were precipitated at 5000*g* for 10 min and washed with minimal medium A. The washed cells were diluted 100-fold with 5 mL of minimal medium containing 15 μg/mL ampicillin and 0.5% glucose or 0.5% glycerol and then grown aerobically at 37 °C in a test tube. The aerobic growth was monitored by the absorbance change at 650 nm with a Coleman Junior IIA spectrophotometer for about 10 h, and the doubling time was calculated graphically from a curve corresponding to the logarithmic phase of the growth.

Purification of Cytochrome bo. The wild-type enzyme was purified from strain GO103/pMFO2 (*cyo*$^+$ Δ*cyd*/*cyo*$^+$ Ap^r) (*10*), and the mutant enzymes were from strain ST4533 (Δ*cyo cyd*$^+$) harboring the pMFO9 derivatives as described previously (*25*). The purified enzymes in 50 mM Tris-HCl (pH 7.4) containing 0.1% sucrose monolaurate SM-1200 (Mitsubishi-Kagaku Foods Corp., Tokyo) were concentrated to about 0.2 mM by ultrafiltration with a Centriprep 100 (Amicon).

Model Building of Subunit I. Using 40% identity of the amino acid sequence of subunit I aligned with that of cytochrome *c* oxidase from *Paracoccus denitrificans*, whose crystal structure has been determined (*11*), homology modeling of subunit I from residue 44 to 563 was made following the conventional method described previously (*26*). There are four deletions, between residues 94 and 95, between 120 and 121, between 160 and 161, and between 165 and 166, and one insertion, between 533 and 535. Backbone structures for these residues were constructed by the loop-search method, using the backbone structures of other proteins (*26*). Assuming that the conserved amino acid residues have the same side-chain conformations as those in the crystal structure, the side-chain rotamer conformations of all the other residues were modeled as those in the energy-minimum conformation of the whole molecule after calculation of the dead-end elimination method (*27*). Finally, the entire structure was optimized without bad contacts and with the position restraints of the atoms in conserved residues, Cu_B, and the two hemes, using a molecular mechanics program PRESTO (*28*) with an AMBER all-atom force field (*29*).

Miscellaneous. DNA manipulations and all other analytical procedures are as described (*10, 13, 14*). Measurements of UV−visible (*13*), EPR, FTIR (*10*), and resonance Raman (*25*) spectra and Q_1H_2 oxidase activity (*14*) were carried out as described previously. Cytochrome *o* was determined from CO binding diffrence spectra using a molar extinction coefficient of 206 000 (T. Mogi, unpublished results). Heme content was determined by pyridine hemochromogen method and calculated as a sum of hemes *b* and *o* using a molar extinction coefficient for heme *b* (*10*). Composition of hemes bound to the enzyme (heme *b* to heme *o* ratio) was analyzed by reverse-phase HPLC (*10*). Copper content was determined by inductively coupled plasma atomic emission spectrophotometry with a SPS 1200VR plasma spectrometer (Seiko Instrument Inc., Tokyo). Restriction endonucleases and other enzymes for DNA manipulation were purchased from Takara Shuzo Co. (Kyoto) or New England Biolabs. Other chemicals are commercial products of analytical grade.

RESULTS

Effect of Mutations on the Catalytic Activity of Mutant Enzymes. In cytochrome *bo*, a total of 19 aromatic amino acid residues are conserved in putative transmembrane helices or at the boundary of the membrane of subunit I (Figure 3). To examine their structural and functional roles, we individually substituted Phe^{112} and Phe^{113} (helix II), Trp^{147} (III), Phe^{208} (IV), Trp^{280}, Tyr^{288}, and Phe^{295} (VI), Trp^{331} and Phe^{336} (loop VII−VIII), Phe^{347} and Phe^{348} (helix VIII), Phe^{391} (IX), Phe^{420} (X) by Leu, Tyr^{61} (I) and Trp^{282} (VI) by Phe, and Phe^{415} (X) by Trp (Figure 1). Phagemid pCYOF9, where six unique restriction sites have been introduced in the present study, facilitated site-directed mutagenesis of the subunit I gene (Figure 2). The largest restriction fragment whose nucleotide sequence should be confirmed by DNA sequencing is now only 0.29 kb (the *Mlu*I−*Eco*81I fragment), instead of 1.2 kb (the *Afl*III−*Spl*I fragment) in pCYOF4 (*13*). Mutations in the pCYOF9 derivatives were confirmed by direct plasmid sequencing and were introduced into the single-copy vector pMFO4 by subcloning of the *Nhe*I−*Eco*RI fragment to produce the pMFO9 derivatives.

The catalytic activity of the mutant enzymes was estimated in vivo by measuring the aerobic growth rates of the terminal oxidase-deficient strain ST2592 harboring the mutant pMFO9. Defective mutants cannot grow aerobically on nonfermentable carbon sources but can grow on glucose via glycolysis. All the mutants except Y288L,[3] W331L, and F348L grew in both media via oxidative phosphorylation, indicating that these mutations did not affect the in vivo activity (Table 1). On the other hand, the Y288L, W331L, and F348L mutants and the vector control strain, ST2592, harboring pHNF2 (*34*) failed to grow in minimal-glycerol medium. Notably, doubling time of W280L in the same medium was 2-fold slower than the wild-type control (Table 1). Subsequently, the defective mutant enzymes, W280L, Y288L, W331L, and F348L, were isolated from cytoplasmic membranes of ST4533 (Δ*cyo cyd*$^+$) harboring the mutant pMFO9. Q_1H_2 oxidase activity of W280L and W331L was reduced to two-thirds and one-fifth of the wild-type level, respectively (Table 2). In Y288L and F348L, the oxidase activity was negligibly low (<1%).

Effects of Mutations on Redox Difference Spectra. Dithionite-reduced minus air-oxidized difference spectra of the mutant enzymes were recorded at 77 K and showed a minor perturbation in the amplitudes of the split α peak of cytochrome $b_{563.5}$ in the W331L and F348L mutants (Figure 4). In the second-order finite difference spectra, the 555.5-nm peak further splits into 554.2 and 557.1 nm in the wild type and 554.8 and 556.6 nm in W280L (data not shown). In W331L and F348L, the 555.5-nm peak was shifted to 555.2 and 554.9 nm, respectively (data not shown).

Effects of Mutations on CO Binding to the Binuclear Center. CO binding UV−visible difference spectra of the

[3] The designations for mutants make use of the standard one-letter abbreviations for amino acids. Thus, Y288L signifies the mutant in which tyrosine at position 288 in subunit I has been substituted by leucine. *E. coli* numbering of amino acid residues is used throughout this work.

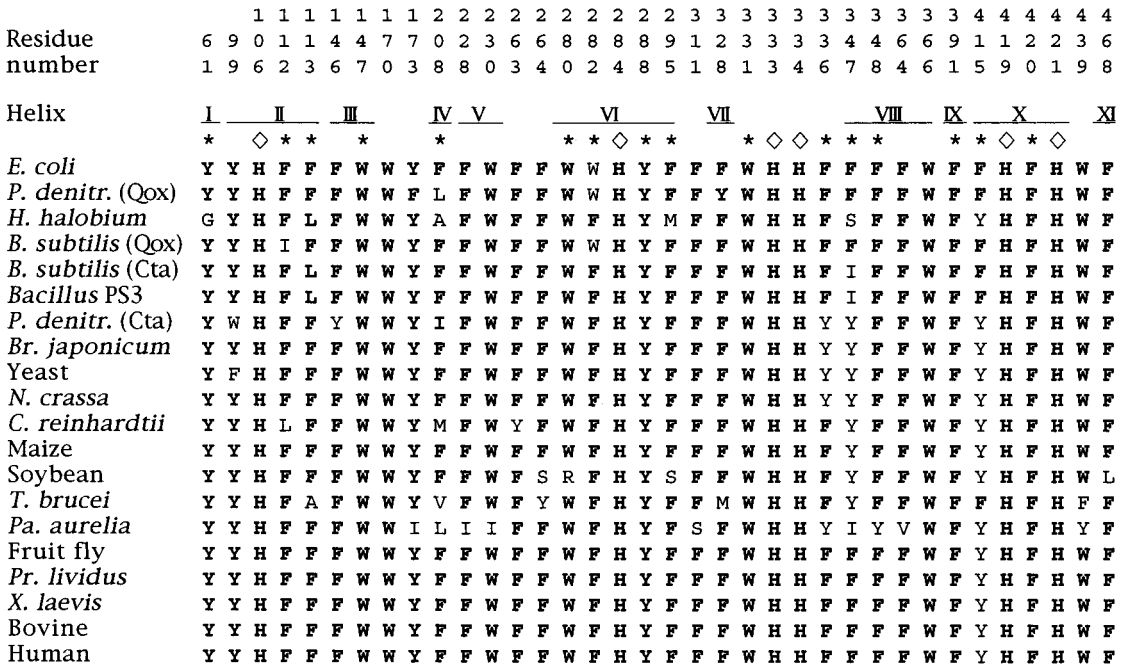

FIGURE 3: Sequence alignment of the conserved aromatic amino acid residues in subunit I of the heme−copper respiratory oxidase superfamily. Amino acid sequences aligned are quinol oxidases [cytochrome *bo* from *E. coli*, cytochrome ba_3 from *P. denitrificans* and *Bacillus subtilis* (QoxB)] and cytochrome *c* oxidases [cytochrome caa_3 from *B. subtilis* (CtaD) and thermophilic *Bacillus* PS3 and cytochrome aa_3 from *Halobacterium salinarium*, *Bradyrhizobium japonicum*, *P. denitrificans*, yeast, *Neurospora crassa*, *Chlamydomonas reinhardtii*, maize, soybean, *Trypanosoma brucei*, *Paramecium aurelia*, *Drosophila melanogaster* (fruit fly), *Paracentrotus lividus*, *Xenopus laevis*, bovine, and human (*13*, *30*−*33*)]. The numbering refers to the *E. coli* sequence. The aromatic amino acid residues altered in this study are marked by asterisks. The invariant histidines are marked by diamonds. Highly conserved residues are indicated by boldface type.

Table 1: Aerobic Growth Rates of the Mutant Strains[a]

mutant	location of mutations	doubling time (h)	
		glucose	glycerol
wild type		1.6	2.5
control		2.1	*b*
Y61F	helix I	1.9	2.6
F112L	helix II	1.7	2.4
F113L	helix II	1.8	2.6
W147L	helix III	1.8	2.8
F208L	helix IV	2.0	2.3
W280L	helix VI	1.9	5.8
W282F	helix VI	1.8	2.6
Y288L	helix VI	1.7	*b*
F295L	helix VI	1.7	2.8
W331L	loop VII−VIII	1.9	*b*
F336L	loop VII−VIII	1.8	2.9
F347L	helix VIII	1.7	2.8
F348L	helix VIII	1.8	*b*
F391L	helix IX	1.9	2.7
F415W	helix X	1.7	2.8
F420L	helix X	1.8	2.9

[a] The terminal oxidase-deficient mutant ST2592 harboring wild-type pMFO9 (wild-type), a vector pHNF2 (control), or the mutant pMFO9 was grown aerobically in minimal-ampicillin medium containing either 0.5% glucose or 0.5% glycerol as sole carbon source. Doubling time was determined as described in Materials and Methods. [b] No growth.

mutant enzymes showed typical features for cytochrome *o* (Figure 5). However, we noticed that a peak and a trough in Y288L were both 3 nm red-shifted as compared to the wild type, as found in heme *o* synthase mutants which produced the heme *bb*-type enzyme (*35*−*38*). Cytochrome *bb*-type enzymes completely lost quinol oxidase activity (<0.1%) and reduced CO binding activity to a fourth of the wild-type level (*36*). Reverse-phase HPLC analysis of the bound hemes revealed that the Y288L mutation specifically substituted heme *b* for heme *o* at the high-spin heme binding site (Table 2). Y288L and F348L almost completely lost their oxidase activities although they retained 14% and 7.5%, respectively, of the CO binding activity (Figure 5, Table 2). Metal analysis demonstrated that these mutations reduced the amounts of bound copper ions to 17% and 9%, respectively (Table 2). The W280L mutation reduced the CO binding activity to 41% of the wild-type level (Figure 5), which was comparable to Q_1H_2 oxidase activity (67%) (Table 2). W331L retained Cu_B (14%) and CO binding activity (12%) (Table 2, Figure 5). Resonance Raman spectra of the CO-bound enzymes revealed that the Fe−CO stretching mode at 523 cm^{-1} of the wild-type enzyme was shifted to 494 cm^{-1} in Y288L, W331L, and F348L (Figure 6), which was similar to that found in the Cu_B-deficient mutant H333A (*25*). FTIR spectra of the CO-bound enzymes showed that the C−O stretching mode at 1959.5 cm^{-1} of the wild type was shifted to higher wavenumbers, 1972, 1969 and 1958, and 1969 cm^{-1} in Y288L, W331L, and F348L, respectively (Figure 7), as found in the Cu_B-deficient mutant (*25*). Upon normalization of the amplitude of EPR spectra of the air-oxidized enzymes based on the $g = 3$ low-spin signal, we found that the $g = 6.0$ signal of high-spin heme increased 3-, 2-, and 36-fold in Y288L, W331L, and F348L and the $g = 3.7$ signal attributable to spin−spin exchange coupling was lost in these mutant oxidases (Figure 8), suggesting the perturbation at the binuclear center. Since the F348L mutation completely eliminated bound copper ions in the cytoplasmic membranes (data not shown), Phe^{348} seems to interact with one of the Cu_B ligands in loop VII−VIII.

Effects of Mutations on CN Binding to the Binuclear Center. CN-binding spectra of the air-oxidized enzymes

Table 2: Properties of the Purified Mutant Oxidases[a]

mutant	Q_1H_2 oxidase (e^-/s)	content (nmol/mg of protein)			heme *b*:heme *o*
		cyt *o*	Cu	heme	
wild type	853 (100)[b]	6.00 (100)	6.78 (100)	11.9 (100)	1.05:0.95
W280L	573 (67)	2.44 (41)	5.45 (80)	9.4 (79)	0.99:1.01
Y288L	2.3 (0.3)	0.81 (14)	1.18 (17)	7.4 (62)	1.87:0.13
W331L	158 (19)	0.70 (12)	0.93 (14)	2.1 (18)	1.26:0.74
F348L	4.8 (0.6)	0.45 (7.5)	0.58 (9)	2.5 (21)	1.26:0.74

[a] Q_1H_2 oxidase activity was determined at 25 °C at a substrate concentration of 0.45 mM. Contents of cytochrome *o*, copper, and heme were determined as described in Materials and Methods. Hemes extracted from the enzyme were analyzed by reverse-phase HPLC, and heme *b* to heme *o* ratios were normalized to a total heme value of 2.0. [b] Percent control values are indicated in parentheses.

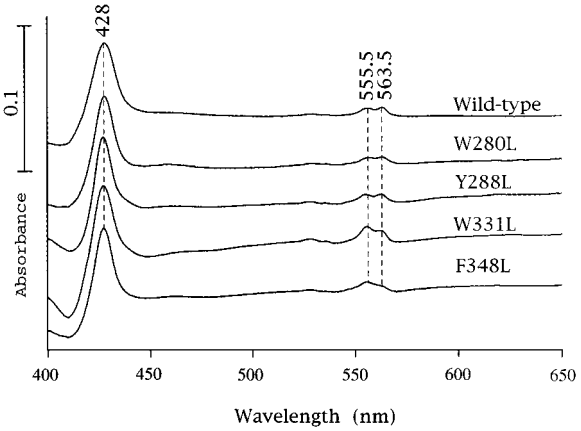

FIGURE 4: Dithionite-reduced minus air-oxidized difference spectra of the wild-type, W280L, Y288L, W331L, and F348L mutant oxidases at 77 K. UV−visible spectra of 5 μM enzyme solution were recorded with a Shimadzu UV-3000 spectrophotometer at 77 K, with a spectral bandwidth of 1 nm and a light path of 2 mm. The scanning rate was 50 nm/min.

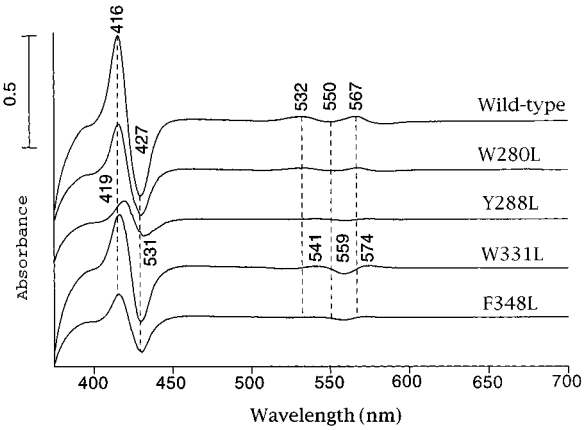

FIGURE 5: CO binding difference spectra of mutant cytoplasmic membranes. Spectra of 2.5 μM enzyme solution were recorded at room temperature with a light path of 1 cm. Other details are described in the legend to Figure 4.

showed that the Soret peak was shifted from the 419 nm wild-type value to 425 and 423 nm in Y288L and W331L, respectively (data not shown). The α region of W331L and F348L showed minor perturbations. FTIR difference spectra of the air-oxidized CN-bound enzymes showed that the C−N stretching mode of the Fe^{3+}−CN−Cu_B structure at 2146 cm^{-1} (*10*) shifted to 2154 and 2127 cm^{-1} in W331L and F348L, respectively, and was absent in Y288L (data not shown). The bridge structure was perturbed in W331L, and the cyanide complex of F348L is likely to have an Fe^{3+}−CN structure (*10*).

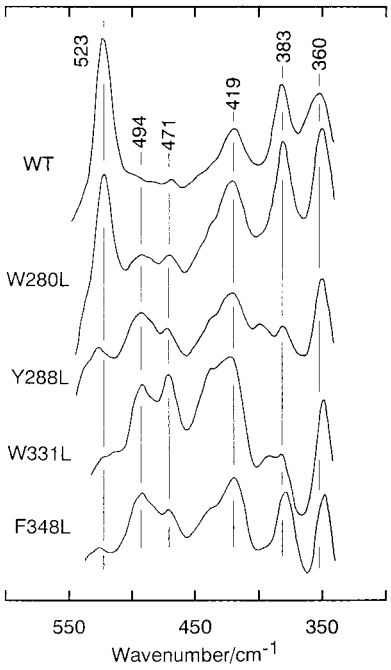

FIGURE 6: Resonance Raman spectra of ferrous CO complexes of the wild-type, W280L, Y288L, W331L, and F348L mutant oxidases. Raman scattering was obtained by excitation with the 406.7 nm line of a Kr^+ laser (Spectra Physics Model 164-01) with a laser power of 5 mW at the sample point. Spectra were recorded with a Jasco R-800UV Raman spectrometer using a spinning cell. The data acquisition time was 300 s.

DISCUSSION

The *E. coli* cytochrome *bo* is the best system for molecular biological studies on the heme−copper respiratory oxidases. Previous studies on subunit I have succeeded in identifying the axial ligands for the redox metal centers and key residues in proton translocation (*7*, *8*, *38*). Side chains of the aromatic amino acid residues may participate in long-range electron transfer between the metal centers (*20*, *21*) or provide a binding pocket for the prosthetic groups (*22*). In bacterial photosynthetic reaction centers, the primary electron transfer from the special pair of (bacterio)chlorophylls to (bacterio)-pheophytin is mediated by a Tyr residue (*39*, *40*). Alternatively, aromatic amino acid residues may provide a tightly packed hydrophobic environment for the buried portion of hemes or a $\pi-\pi$ interaction to stabilize a chromophore. In yeast iso-1-cytochrome *c*, aromatic residues stabilize a bound heme *c* molecule via H-bonds (*41*) and the conformation of the active protein structure by providing a large hydrophobic group at the proper location (*42*). Residues 84−90, including Phe^{87}, are essential for maintenance of the heme environment, provision of an optimal polypeptide medium along the path

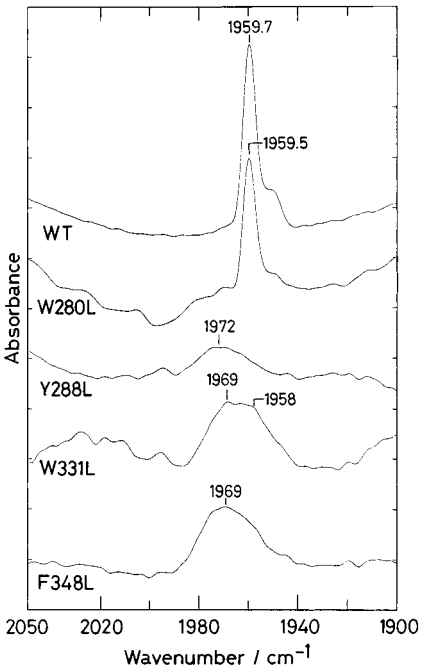

FIGURE 7: FTIR spectra of ferrous CO complexes of the wild-type, W280L, Y288L, W331L, and F348L mutant oxidases. Reduced CO-bound minus air-oxidized difference spectra were taken at 10 °C with a Perkin-Elmer Model 1850 FTIR spectrophotometer using CaF_2 cells with a light path of 51 μm. The nominal spectral resolution was 4 cm^{-1}.

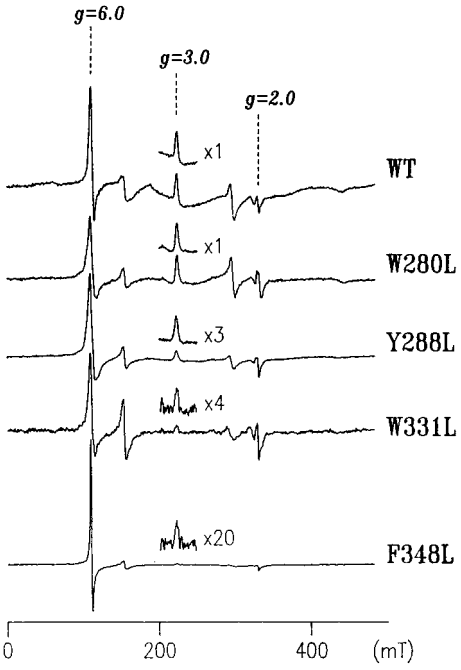

FIGURE 8: EPR spectra of the wild-type (WT), W280L, Y288L, W331L, and F348L mutant oxidases under air-oxidized conditions. Spectra of 0.1 mM oxidase solution were recorded at 5 K with a home-built EPR spectrometer equipped with an Oxford flow cryostat (ESR-900). Experimental conditions were as follows: microwave frequency, 9.23 GHz; modulation frequency, 100 kHz; microwave power, 5 mW; modulation amplitude, 0.5 mT; accuracy of the *g*-values, ± 0.01.

of electron transfer, and formation of interactions at the contact interface in complexes with redox partners (*43*).

To explore functional roles of the conserved aromatic amino acid residues in cytochrome *bo* subunit I, we have individually replaced 16 residues in transmembrane helices

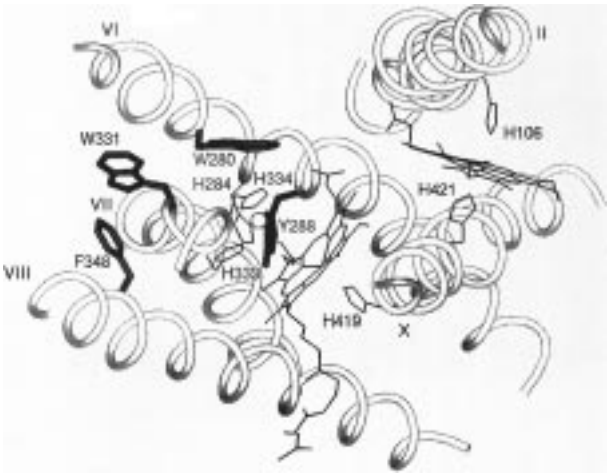

FIGURE 9: A projection model of subunit I of cytochrome *bo* showing interactions of the conserved aromatic amino acid residues with the redox metal centers.

(or at the boundary of the membrane) with Leu, Phe, or Trp (Figures 1 and 3). We found that the Leu substitutions of Phe^{112} (helix II), Phe^{113} (II), Trp^{147} (III), Phe^{208} (IV), Phe^{295} (VI), Phe^{336} (VII), Phe^{347} (VIII), Phe^{391} (IX) and Phe^{420} (X), the Phe substitutions of Tyr^{61} (I) and Trp^{282} (VI), and the Trp substitution of Phe^{415} (X) did not affect the catalytic activity. In contrast, the Leu substitutions of Trp^{280} (VI), Tyr^{288} (VI), Trp^{331} (VII), and Phe^{348} (VIII), which are all present near the heme−copper binuclear center (*7*, *8*, *11*, *44*) (Figure 9), resulted in reduction or loss of the catalytic activity that was associated with perturbation of the binuclear center (Table 2). Our findings support the functional or structural importance of subunit I.

Crystallographic studies of cytochrome *c* oxidases suggest that Tyr^{61} can H-bond with Ser^{145} (III) and the fixed water molecules at Asn^{142} and Gly^{200} (Ser in *P. denitrificans* and bovine) and is part of a proton channel (*11*, *44*). The Y61F mutant was still functional and Ser at position 200 is not conserved in the *E. coli* enzyme, suggesting that Tyr^{61} does not have an obligatory role in proton translocation. Phe^{420} and Ile^{424} (Met in *P. denitrificans* and Leu in bovine) could mediate heme-to-heme electron transfer with their side chains, which are in contact with both hemes (*11*, *12*). The F420L mutation did not affect the catalytic activity and position 424 is not conserved in the heme−copper terminal oxidases; therefore, long-range electron transfer through side chains at positions 420 and 424 is less likely. Tyrosines or tryptophan expected to be near propionate groups of the hemes (*44*, *45*) are substituted in cytochrome *bo* (Leu^{414}, Phe^{415}, and Leu^{483}) except Tyr^{99}, and the F415W mutation did not affect the in vivo activity. Therefore, except for Tyr^{99} (Trp in *P. denitrificans*), those other residues are less likely to stabilize the heme propionates in cytochrome *bo*. Aromatic side chains of Phe and Trp may provide a hydrophobic channel for dioxygen transfer to the binuclear center (*44*), and Phe^{112}, Trp^{282}, Trp^{170}, and Trp^{280} are conserved in cytochrome *bo* (Figure 3). However, Phe at position 279 is substituted by Ile in cytochrome *bo* and the F112L and W282F mutations did not affect the in vivo catalytic activity. Thus, this proposal remains to be proven.

Trp^{280}. In the crystal structures of cytochrome *c* oxidases (*11*, *12*), the indole ring of Trp^{280} is in van der Waals distance parallel to the imidazole ring of His^{334} (Figure 9); such a

$\pi-\pi$ interaction may stabilize Cu_B, which is ligated by His^{284}, His^{333}, and His^{334} (*7*, *8*, *11*, *25*, *44*). Trp^{280} is also suggested as part of a channel for pumped protons (*11*) and dioxygen transfer (*44*). The W280L mutation incresed the generation time for aerobic growth on a nonfermentable carbon source 2-fold and also reduced Q_1H_2 oxidase activity to 67% of the wild-type level (Tables 1 and 2). UV−visible and resonance Raman spectra of the CO-bound form indicated that the binuclear center was slightly perturbed in the W280L mutant (Figures 5 and 6). Svensson et al. (1996) purified the W280F mutant enzyme in Triton X-100 and *N*-lauroyl sarcosinate and found that the mutation reduced Q_2H_2 oxidase activity to 6% of the wild-type level and impaired proton uptake without affecting electron transfer (*46*). The difference in phenotypes of these two mutations could be attributable to differences in substituting amino acid residues or detergents used for purification. Triton X-100 is known to remove noncatalytic subunits (*47*) and a tightly bound Q_8 (*48*, *49*) from cytochrome *bo*.

Tyr^{288}. Previous spectroscopic studies on mutants suggest that Tyr^{288} is a possible ligand of Cu_B (*7*, *8*, *50*). On the basis of resonance Raman studies, Tyr^{288} was proposed to be involved in proximal ligand exchange between Tyr^{288} and His^{419} at high-spin heme (*45*). However, crystallographic studies on cytochrome *c* oxidases (*11*, *12*) disproved these possibilities. Tyr^{288} can form an H-bond with His^{284} and the hydroxyethylfarnesyl group of high-spin heme; therefore, it may mediate electron transfer between high-spin heme and Cu_B (*12*). In addition, Tyr^{288} may deliver a proton from the channel to dioxygen at the binuclear center (*11*, *51*).

The Y288L (Table 2) and Y288F (*38*) mutations replaced heme *o* at the high-spin heme binding site with heme *b* and reduced Q_1H_2 oxidase activity (0.3% of the control level), CO binding activity (22%), and the level of bound copper ions (32%). UV−visible, resonance Raman, and FTIR spectra of the ferrous CO-bound and ferric CN-bound forms showed that the binuclear center was severely perturbed by the Leu substitution (Figures 5−7). EPR spectra of the air-oxidized enzyme also indicated a perturbation at high-spin heme (Figure 8). Thomas et al. (*52*) reported that Y288F, Y288A, Y288H, and Y288S were found to be nonfunctional from a genetic complementation test. Flash photolysis studies showed that the CO rebinding rate decreased 5-fold in the Tyr^{288} mutant membranes (*50*), and FTIR spectroscopy revealed that the Tyr^{288} mutations eliminated Cu_B from the mutant enzymes (*52*). The purified Y288F mutant displayed a lower overall activity (<1%) and a disruption of oxygen reduction (*38*, *46*). These data support the interactions with the hydroxyethylfarnesyl group of high-spin heme and His^{284}, the Cu_B ligand (Figure 9). Thus, we conclude that Tyr^{288} is crucial for catalytic function at the binuclear center.

Trp^{331}. Trp^{331} is highly conserved in loop VII−VIII (Figure 3) and is close to one of the Cu_B ligands, His^{334}. In the crystal structure of bacterial cytochrome *c* oxidase, the side chain of Trp^{331} is in van der Waals distance to Asn^{277} (VI), Thr^{320} (VII), and Phe^{348} (VIII) (*11*) (Figure 9). Positions 277 and 320 are His and Met, respectively, in the *P. denitrificans* and bovine oxidases. Time-resolved resonance Raman studies on the reaction of the reduced enzyme with dioxygen postulated that one or more of the Trp residues (Trp^{280}, Trp^{282}, and/or Trp^{331}) or Tyr^{288} provides electrons to the binuclear center without passing through heme *b* (*53*). The W331L mutant enzyme cannot support aerobic growth and had reduced Q_1H_2 oxidase (19%) and CO binding (67%) activities. Spectroscopic characterizations of the air-oxidized, ferrous CO-bound and ferric CN-bound enzymes indicated that the binuclear center was severely perturbed even though it can retain Cu_B. Our data indicate that the side chain of Trp^{331} is part of a binding pocket for the binuclear metal center (Figure 9).

Phe^{348}. Phe^{348} in helix VIII is highly conserved in the heme−copper respiratory oxidase superfamily (Figure 3) and has been proposed to face the binuclear center (*8*). The functional or structural importance of Phe^{348} was not realized in crystallographic studies on cytochrome *c* oxidases (*11*, *44*). We found that the F348L mutation severely reduced Q_1H_2 oxidase (0.6%) and CO binding (36%) activities and the enzyme copper content (46%) and greatly enhanced the $g = 6$ high-spin signal of the air-oxidized enzyme (Table 2, Figures 5 and 8), as found in the Cu_B-deficient mutant (*54*, *55*). Resonance Raman and FTIR studies support the perturbation at the binuclear center. The side chain of Phe^{348} is in van der Waals distance to Trp^{331}, Leu^{332}, and Ala^{340} (loop VII−VIII), and Phe^{347} and Thr^{351} (VIII) in bacterial cytochrome *c* oxidase (*11*). Among them, the aromatic amino acid residues are highly conserved at positions 331 and 347. These observations suggest that the aromatic side chains at positions 331, 347, and 348 are essential for forming an active form of the binuclear center (Figure 9).

In conclusion, the present studies demonstrated that Trp^{280}, Tyr^{288}, Trp^{331}, and Phe^{348} in subunit I are indispensable for the catalytic function(s) of cytochrome *bo* and suggested that they are involved in assembly and/or function of the heme−copper binuclear center. Spectroscopic studies on intramolecular electron transfer and on the protonation state of Tyr^{288} during the catalytic cycle should further provide a clue for their functional role(s).

ACKNOWLEDGMENT

We thank R. B. Gennis (University of Illinois) for the *E. coli* strain GO103, M. Ohno (Eisai Co. Ltd., Tsukuba, Japan) for Q_1, E. Yoshimura (University of Tokyo) for copper analysis, H. Shimizu, S. Harada, and Y. Satow (University of Tokyo) for use of their computer graphics facility, and H. Michel (Max Planck Institute) for the coordinates of cytochrome *c* oxidase from *P. denitrificans*.

REFERENCES

1. Kranz, R. G., and Gennis, R. B. (1983) *J. Biol. Chem. 258*, 10614−10621.
2. Matsushita, K., Patel, L., and Kaback, H., R. (1984) *Biochemistry 23*, 4703−4714.
3. Kita, K., Kasahara, M., and Anraku, Y. (1982) *J. Biol. Chem. 257*, 7933−7935.
4. Puustinen, A., Finel, M., Virkki, M., and Wikström, M. (1989) *FEBS Lett. 249*, 163−167.
5. Saraste, M. (1990) *Q. Rev. Biophys. 23*, 331−366.
6. Castresana, J., Lübben, M., Saraste, M., and Higgins, D. G. (1994) *EMBO J. 13*, 2516−2525.
7. Hosler, J. P., Ferguson-Miller, S., Calhoun, M. W., Thomas, J. W., Hill, J., Lemieux, L., Ma, J., Georgiou, C., Fetter, J., Shapleigh, J., Tecklenburg, M. M. J., Babcock, G. T., and Gennis, R. B. (1993) *J. Bioenerg. Biomembr. 25*, 121−136.
8. Mogi, T., Nakamura, H., and Anraku, Y. (1994a) *J. Biochem. (Tokyo) 116*, 471−477.

9. Salerno, J. C., Bolgiano, B., Poole, R. K., Gennis, R. B., and Ingledew, J. W. (1990) *J. Biol. Chem. 265*, 4364−4368.
10. Tsubaki, M., Mogi, T., Anraku, Y., and Hori, H. (1993) *Biochemistry 32*, 6065−6072.
11. Iwata, S., Ostermeier, C., Ludwig, B., and Michel, H. (1995) *Nature 376*, 660−669.
12. Tsukihara, T., Aoyama, H., Yamashita, E., Tomizaki, T., Yamaguchi, H., Shinzawa-Itoh, K., Nakashima, R., Yaono, R., and Yoshikawa, S. (1995) *Science 269*, 1069−1074.
13. Minagawa, J., Mogi, T., Gennis, R. B., and Anraku, Y. (1992) *J. Biol. Chem. 267*, 2096−2104.
14. Sato-Watanabe, M., Mogi, T., Miyoshi, H., Iwamura, H., Matsushita, K., Adachi, O., and Anraku, Y. (1994a) *J. Biol. Chem. 269*, 28899−28907.
15. Sato-Watanabe, M., Mogi, T., Ogura, T., Kitagawa, T., Miyoshi, H., Iwamura, H., and Anraku, Y. (1994b) *J. Biol. Chem. 269*, 28908−28912.
16. Sato-Watanabe, M., Itoh, S., Mogi, T., Matsuura, K., Miyoshi, H., and Anraku, Y. (1995) *FEBS Lett. 374*, 265−269.
17. Welter, R., Gu, L.-Q., Yu, L., Yu, C.-A., Rumbley, J., and Gennis, R. B. (1994) *J. Biol. Chem. 269*, 18834−18838.
18. Svensson-Ek, M., and Brzezinski, P. (1997) *Biochemistry 36*, 5425−5431.
19. Woodruff, W. H. (1993) *J. Bioenerg. Biomembr. 25*, 177−188.
20. Poulos, T. L., and Kraut, J. (1980) *J. Biol. Chem. 255*, 10322−10330.
21. Wendoloski, J. J., Batthew, J. B., Weber, P. C., and Salemme, F. R. (1987) *Science 238*, 794−797.
22. Mogi, T., Marti, T., and Khorana, H. G. (1989) *J. Biol. Chem. 264*, 14197−14201.
23. Minagawa, J., Nakamura, H., Yamato, I., Mogi, T., and Anraku, Y. (1990) *J. Biol. Chem. 265*, 11198−11203.
24. Davis, B. D., and Mingioli, E. S. (1959) *J. Bacteriol. 60*, 17−28.
25. Uno, T., Mogi, T., Tsubaki, M., Nishimura, Y., and Anraku, Y. (1994) *J. Biol. Chem. 269*, 11912−11920.
26. Nakamura, H., Katayanagi, K., Morikawa, K., and Ikehara, M. (1991) *Nucleic Acids Res. 19*, 1817−1823.
27. Tanimura, R., Kidera, A., and Nakamura, H. (1994) *Protein Sci. 3*, 2358−2365.
28. Morikami, M., Nakai, T., Kidera, A., Saito, M., and Nakamura, H. (1992) *Comput. Chem. 16*, 243−248.
29. Weiner, S. J., Kollman, P. A., Nguyen, D. T., and Case, D. (1986) *J. Comput. Chem. 7*, 230−252.
30. Ishizuka, M., Machida, K., Shimada, S., Mogi, A., Tsuchiya, T., Ohmori, T., Souma, Y., Gonda, M., & Sone, N. (1990) *J. Biochem. (Tokyo) 108*, 866−873.
31. Denda, K., Fujiwara, T., Seki, M., Yoshida, M., Fukumori, Y., and Yamanaka, T. (1991) *Biochem. Biophys. Res. Commun. 181*, 316−322.
32. Santana, M., Kunst, F., Hullo, M. F., Rapoport, G., Danchin, A., and Glaser, P. (1992) *J. Biol. Chem. 267*, 10225−10231.
33. Richter, O.-M. H., Tao, J.-S., Turba, A., and Ludwig, B. (1994) *J. Biol. Chem. 269*, 23079−23086.
34. Nakamura, H., Mogi, T., and Anraku, Y. (1997) *J. Biochem. (Tokyo) 122*, 415−421.
35. Saiki, K., Mogi, T., and Anraku, Y. (1992) *Biochem. Biophys. Res. Commun. 189*, 1491−1497.
36. Saiki, K., Mogi, T., Hori, H., Tsubaki, M., and Anraku, Y. (1993) *J. Biol. Chem. 268*, 26927−26934
37. Mogi, T., Saiki, K., and Anraku, Y. (1994b) *Mol. Microbiol. 14*, 391−398.
38. Kawasaki, M., Mogi, T., and Anraku, Y. (1997) *J. Biochem. (Tokyo) 122*, 422−429.
39. Barry, B. A., and Babcock, G. T. (1987) *Proc. Natl. Acad. Sci. U.S.A. 84*, 7099−7103.
40. Yeates, T. O., Komiya, H., Chirino, A., Rose, D. C., Allen, J. P., and Feher, G. (1988) *Proc. Natl. Acad. Sci. U.S.A. 85*, 7993−7997.
41. Pielak, G. J., Concar, D. W., Moore, G. R., & Williams, R. J. P. (1987) *Protein Eng. 1*, 83−88.
42. Schweingruber, M. E., Stewart, J. W., and Sherman, F. (1979) *J. Biol. Chem. 254*, 4132−4143.
43. Liang, N., Pielak, G. J., Mauk, A. G., Smith, M., and Hoffman, B. M. (1987) *Proc. Natl. Acad. Sci. U.S.A. 84*, 1249−1252.
44. Tsukihara, T., Aoyama, H., Yamashita, E., Tomizaki, T., Yamaguchi, H., Shinzawa-Itoh, K., Nakashima, R., Yaono, R., and Yoshikawa, S. (1996) *Science 272*, 1136−1144.
45. Rousseau, D. L., Ching, Y.-C., and Wang, J. (1993) *J. Bioenerg. Biomembr. 25*, 165−176.
46. Svensson-Ek, M., Thomas, J. W., Gennis, R. B., Nilsson, T., and Brzezinski, P. (1996) *Biochemistry 35*, 13673−13680.
47. Kita, K., Konishi, K., and Anraku, Y. (1984) *J. Biol. Chem. 259*, 3368−3374.
48. Puustinen, A., Verkhovsky, M. I., Morgan, J. E., Belevich, N. P., and Wikström, M. (1996) *Proc. Natl. Acad. Sci. U.S.A. 93*, 1545−1548.
49. Rumbley, J. N., Nickels, E. F., and Gennis, R. B. (1997) *Biochim. Biophys. Acta 1340*, 131−142.
50. Brown, S., Moody, A. J., Mitchell, R., and Rich, P. R. (1993) *FEBS Lett. 316*, 216−223.
51. Brown, S., Rumbley, J. N., Moody, A. J., Thomas, J. W., Gennis, R. B., & Rich, P. R. (1994) *Biochim. Biophys. Acta 1183*, 521−532.
52. Thomas, J. W., Calhoun, M. W., Lemieux, L. J., Puustinen, A, Wikström, M., Alben, J. O., and Gennis, R. B. (1994) *Biochemistry 33*, 13013−13021.
53. Wang, J., Rumbley, J., Ching, Y.-C., Takahashi, S., Gennis, R. B., and Rousseau, D. L. (1995) *Biochemistry 34*, 15504−15511.
54. Tsubaki, M., Mogi, T., Hirota, S., Ogura, T., Kitagawa, T., and Anraku, Y. (1994) *J. Biol. Chem. 269*, 30861−30868.
55. Mogi, T., Hirano, T., Nakamura, H., Anraku, Y., and Orii, Y. (1995) *FEBS Lett. 370*, 259−263.

BI971978K